NJC

Accepted Manuscript

This is an *Accepted Manuscript*, which has been through the Royal Society of Chemistry peer review process and has been accepted for publication.

Accepted Manuscripts are published online shortly after acceptance, before technical editing, formatting and proof reading. Using this free service, authors can make their results available to the community, in citable form, before we publish the edited article. We will replace this *Accepted Manuscript* with the edited and formatted *Advance Article* as soon as it is available.

You can find more information about *Accepted Manuscripts* in the Information for Authors.

Please note that technical editing may introduce minor changes to the text and/or graphics, which may alter content. The journal's standard Terms & Conditions and the Ethical guidelines still apply. In no event shall the Royal Society of Chemistry be held responsible for any errors or omissions in this *Accepted Manuscript* or any consequences arising from the use of any information it contains.

ROYAL SOCIETY OF CHEMISTRY

www.rsc.org/njc

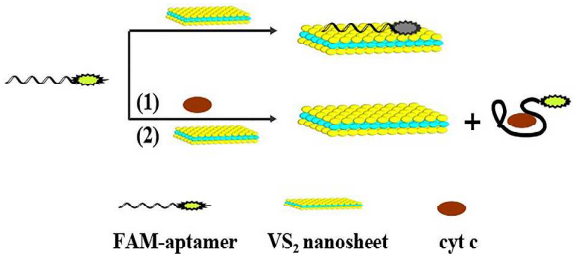

A VS_2/aptamer-based cytochrome c sensor was successfully constructed by first applying the DNA-adsorbing ability/fluorescence-quenching properties of VS_2 in bioanalysis.

A Novel VS_2 Nanosheets-Based Biosensor for Rapid Fluorescence Detection of Cytochrome C

Xuehua Yin, Jin Cai, Hongyan Feng, Zeming Wu, Jianmei Zou, Qingyun Cai*

State Key Laboratory of Chemo/Biosensing and Chemometrics, College of Chemistry and Chemical Engineering, Hunan University, Changsha 410082, China.

*To whom correspondence should be addressed.

E-mail: qycai0001@hnu.edu.cn; qycai0002@gmail.com.

ABSTRACT

A novel ultrasensitive sensing system for rapid fluorescence detection of cytochrome c (cyt c) was proposed by combining aptamer-based bioassay with VS_2 nanosheets. VS_2 nanosheets with high fluorescence quenching ability were synthesized by the solution route. Cyt c-binding aptamer was tagged with the fluorescent dye carboxy fluorescein (FAM), acting as the probe. VS_2 nanosheets can adsorb the probe and quench its fluorescence efficiently. However, the fluorescence of the probe was retained when it was incubated with cyt c and then mixed with VS_2 nanosheets solution. The proposed sensing system shows high selectivity and sensitivity, giving a linear range of 0.75 nM to 50 μM, and a limit of detection of 0.50 nM.

***Keywords**:* VS_2 nanosheets, Cytochrome c, Aptamer, Fluorescence detection, Biosensor

Introduction

Cyt c, containing iron porphyrins as a prosthetic group, is a water-soluble, mitochondrial redox chromo protein and widespread in organisms. Cyt c plays an important physiological role in oxidative phosphorylation.[1, 2] Under normal circumstances, cyt c is located on the crest of mitochondrial membrane in cells, acting as an electron carrier in the mitochondrial intermembrane space between cyt c reductase and cyt c oxidase. However, cyt c can be translocated out from mitochondria to cytosol under various pathological conditions, triggering the activation of caspases and subsequent apoptotic cell death.[3-5] A large number of trials have found that cyt c releasing from mitochondrial intermembrane space to the cytoplasm is the key step in the mitochondria way cells apoptosis[6] and an early sign of apoptosis.[7-9] Thus, this protein has been identified as an important mediator in apoptotic pathways and is used as an information material of apoptosis.[10] Therefore, the measurement of cyt c is of significant importance in better understanding cell apoptosis. Great efforts

have been made so far to detecting cyt c. Conventionally, western blot and enzyme linked immunosorbent assay (ELISA)[11, 12] can be used to effectively determine the amount of cyt c. However, polyclonal antibodies (Abs) against cyt c hardly show a single band in the western blot analysis due to the cross-reactivity of the anti-cyt c Ab that binds to some other proteins, which exhibits poor selectivity. Meanwhile, the signal amplification in ELISA is mediated by enzymatic reaction, which is limited by the availability of substrates. Other analytical methods for cyt c include flow cytometry,[13] electrophoresis,[14] high performance liquid chromatography.[15] Though possessing high sensitivity, most of these methods are somewhat time-consuming, require expensive instrument and complicated sample pretreatment process, therefore are not adaptable to routine analysis. Besides these methods, spectroscopical[16-19] and electrochemical method[20-22] have emerged as alternative tools for rapid and real-time analysis of clinically relevant analytes and gained good detection limits. However, they are vulnerable to interferences caused by other positively charged species present in the samples and hence are not applicable for the measurement of cyt c released in biological systems. Therefore, there is an ever-increasing demand for more simple, selective and economical methods for fast scanning of cyt c in clinic detection and research applications.

Graphene, a two-dimensional nanomaterial, has been extensively used in biological assays.[23-26] Transition metal dichalcogenides (TMDCs), as two-dimensional (2D) layered nanomaterials analogous to graphene, are MX_2-type compounds where M is a transition element from groups IV, V, and VI of the periodic table and X represents the chalcogen species S, Se, and Te.[27-29] Recently, TMDCs have received growing attentions owing to their high specific large surface area and remarkable electronic properties catering for intriguing applications in optoelectronics and energy harvesting.[30-34] Li et al. prepared and applied exfoliated single-layer and multilayer MoS_2 in detecting NO gas and obtained optimistic results.[35] Zhu et al. revealed that MoS_2 nanosheet possesses high fluorescence quenching efficiency and different affinities towards single-stranded DNA (ssDNA) versus double stranded DNA (dsDNA).[36] Yuan et al. synthesized the layered WS_2 nanosheet, which acts as a

platform for easy assembly of biological probes and affords high efficiency to quench the emission of luminophors on or near the surface. This fluorescence assay gained low background and high sensitivity.[37] Xi et al. have recently detected miRNA by combining WS_2 nanosheet based fluorescence quenching with duplex-specific nuclease signal amplification.[38] It becomes obvious that MoS_2 nanosheet and WS_2 nanosheet can act as a nanoplatform to adsorb gas molecules or biomolecules (like ssDNA, dsDNA and RNA) and exhibit a capability for quench luminescence of fluorophores via energy transfer processes. Subsequently, restoration of the fluorescence was expected once upon the introduction of sensing targets, which reacts with DNA probes and alters their molecular conformation leading to weakened physisorption because the nucleobases are shielded by the phosphate backbone in such situations. It is worth mentioning that besides the DNA hybridization, specific aptamer-target recognition can induce dramatic structural switching of the DNA probe.[39-40] So such nanosheets biosensors can also be applied to detect certain proteins when using corresponding aptamer as the probe.

Vanadium disulfide (VS_2), composed of the metal V layers sandwiched between two sulfur layers and stacked together by weak van der Waals interactions, is a typical family member of TMDCs.[41] VS_2 is considered to have great potential for applications in such as sensor,[42] energy storage devices,[43-45] and spintronics.[46-48] Nevertheless, to the best of our knowledge, the biological applications of VS_2 nanosheets have not been explored up to now. Considering that most transition-metal ions possess intrinsic molecule adsorption and fluorescence quenching properties,[49-51] we believe that VS_2 also has potential applications in fluorescence-based detection of biological molecules. What's more, fluorescent method has been proved to be a powerful optical technique for the trace detection of analytes due to its high sensitivity.

In this work, a VS_2 nanosheets-based biosensor was proposed for the first time for fluorescence detection of cyt c with aptamer as recognizer. As we know, aptamers are special functional nucleotide sequences that have been selected towards a large pool of targets with high selectivity and affinity.[52, 53] They are able to bind to targets in a specific manner, analogous to antibody-antigen interactions.[54, 55] Good selectivity as

well as high sensitivity would be gained if aptamer to be used in detecting the specific protein, thanks to its unique character.[56]

Results and discussion

Principle of the sensing system

Long chain of carbohydrates can be adsorbed on the surface of the VS_2 nanosheets based on the researches on TMDCs.[57] Because most of the transition metal ions possess the nature of quenching fluorescence through an energy transfer process, [49-51] nanosheet is expected to possess the same properties and be used to construct a platform for analysis of biological interests based on its properties of fluorescence quenching and adsorption towards biological molecules such as oligomeric nucleotide and polypeptide. The VS_2-based cyt c biosensor is illustrated in Fig. 1.

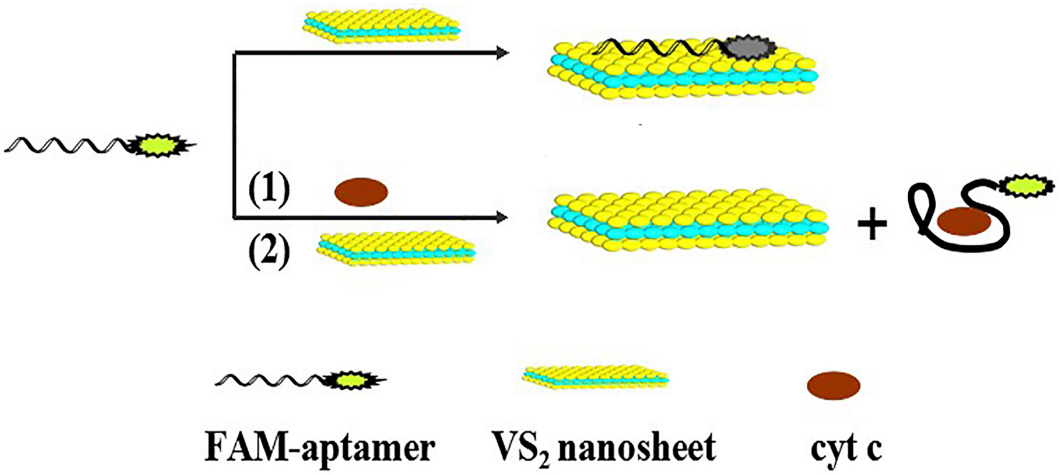

Fig. 1 Schematic representation of the VS_2 nanosheets-based biosensor for rapid fluorescence detection of cyt c.

The fluorescence dye-labeled aptamer is adsorbed on the VS_2 nanosheet via the van der Waals force between nucleobases and the basal plane of VS_2, resulting in the quenching of fluorescence. In the presence of cyt c, the aptamer undergoes adaptive conformational change and adopts a rigid and definite tertiary structure so that it can bind with cyt c.[55] In such a rigid structure, the nucleobases are shielded by the

phosphate backbone leading to weakened physisorption. The fluorescence is restored. As a result, the fluorescence of the probe provides a quantitative readout of the target protein. The combination of VS_2 nanosheets with the aptamer affinities makes the sensing system useful for protein detection.

Characterization of VS_2 nanosheets

VS_2 nanosheets were prepared by firstly synthesizing the $VS_2{\cdot}NH_3$ precursor through hydrothermal method and then exfoliating it into nanosheets. The SEM images of Fig. 2A and 2B clearly shows the flower-like $VS_2{\cdot}NH_3$ precursors and the exfoloated VS_2 nanosheet which is on the Ti substrate. The $VS_2{\cdot}NH_3$ precursors are composed of a large number of nanosheets assembled like flowers (Fig. 2A). While the $VS_2{\cdot}NH_3$ precursors were ultrasonically treated, they became dispersed nanosheets with irregular shapes with an average width of about 300 nm (Fig. 2B). Small particles in the background of Fig. 2B are the surface morphologies of the Ti substrate. The EDS analysis of Fig. 2B shows the characteristic peaks of V and S with an approximate elemental composition of 1:2 (V/S) as shown in the inserted table in Fig. 2C, verifying the desired stoichiometry of the products. The existence of elements Ti is assigned to the titanium substrate. TEM image of VS_2 nanosheets is shown in Fig. 2D. The HRTEM image of VS_2 in Fig. 2E indicates that the interplanar spacing is 0.277 nm which is corresponding to the (100) plane of VS_2 (0.2784 Å). HRTEM investigations in the edge areas of VS_2 are presented in Figure 2F, from which six to seven dark and bright patterns can be readily identified, indicating that the sample was stacked up with six to seven single layers. The interlayer spacing measured in the edge-area HRTEM image was about 0.571 nm, which was also in accordance with the c parameter of VS_2 (0.573 nm).

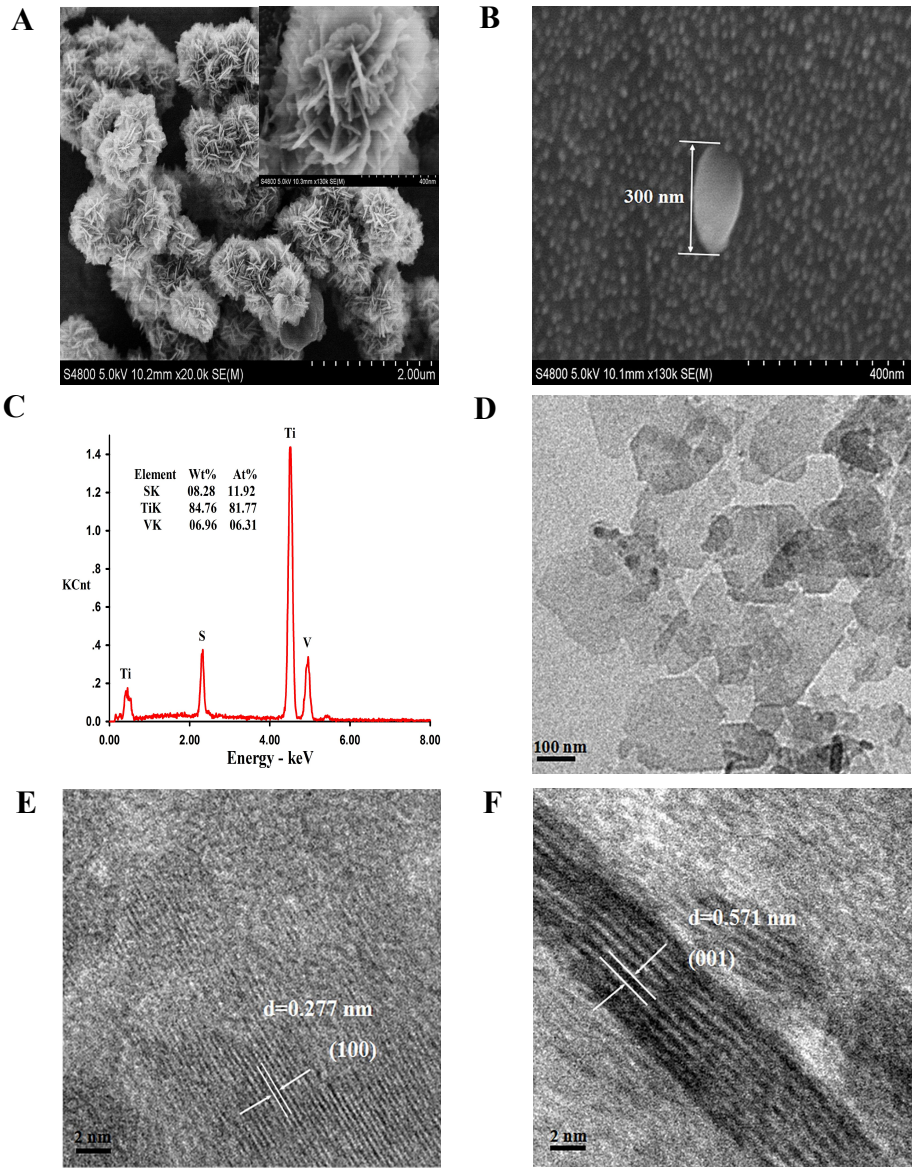

Fig. 2 FE-SEM images of (A) the $VS_2 \cdot NH_3$ precursor and (B) the ultrasonically treated $VS_2 \cdot NH_3$ precursor, a single VS_2 nanosheet is observed on titanium substrate; (C) EDS spectrum of VS_2 nanosheet on titanium substrate; (D)TEM image of VS_2 nanosheets; (E) and (F): HRTEM images of VS_2 nanosheets.

Detection of cyt c

Aptamer which shows favorable binding properties to cyt c [58] was labeled with dye FAM and served as the probe (P1) (FAM-5'-CCGTGTCTGGGGCCGACCGGCGCATTGGGTACGTTGTTGC-3'). As shown in Fig. 3, 81% of the fluorescence of P1 is quenched within 5 min after P1 (30 μL, 1.5 μM) was introduced into VS_2 nanosheets solution (40 μL, 0.4 mg/mL) (comparing curve a with curve d, Fig. 3), demonstrating that VS_2 nanosheet possesses a high fluorescence quenching ability, and the interaction between aptamer and VS_2 nanosheets is fast and strong. The addition of 60 μL cyt c (5×10^{-5} M) results in an enhancement of the fluorescence intensity by 3 times (comparing curve c with curve d, Fig. 3). In the absence of VS_2 nanosheets, however, the combination of P1 with cyt c results in a decrease in fluorescence by 15% (comparing curve a with curve b, Fig. 3). The possible reason would be the change of aptamer structure which resulted in the decrease in fluorescence of the dye.

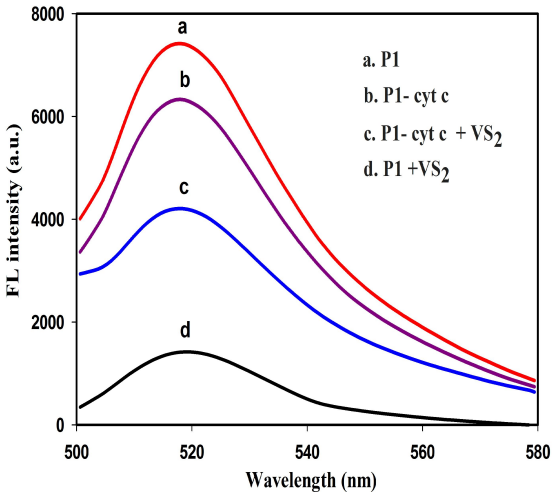

Fig. 3 Fluorescence spectra of P1 and P1-cyt c complex in the absence and presence of VS_2 nanosheets. Excitation and emission wavelengths are at 490 nm and 518 nm, respectively.

Optimization of the experimental conditions

VS_2 nanosheets work as the fluorescence quencher and substrate on which dye-labeled aptamer is adsorbed. The amount of VS_2 nanosheets is therefore a crucial parameter that affects the sensitivity. Fig. 4 shows the dependence of responses on the amount of VS_2 nanosheets with/without the target cyt c. In the absence of cyt c, most of the dye-labeled aptamer (P1) are absorbed on the VS_2 nanosheets resulting in the fluorescence quench. The fluorescence intensity in the absence of cyt c was defined as the background which would be the less the better. While in the presence of cyt c, the dye-labeled aptamer binds with cyt c undergoing adaptive conformational changes,[55] resulting in desorption of the cyt c-aptamer complex. The fluorescence is then restored. As shown in Fig. 4, the fluorescence intensity decreases with increasing the VS_2 nanosheet concentration no matter with or without cyt c. However, there is a maximum on the cyt c-resulted increase in the fluorescence (the largest response/background ratio), at which the VS_2 nanosheet concentration is defined as the optimal concentration (0.4 mg/mL). Ones may notice that in the absence of VS_2 nanosheet, the fluorescence intensity of dye-modified aptamer is higher than that of the cyt c-aptamer complex, indicating that the conformational change of aptamer decreases the fluorescenc

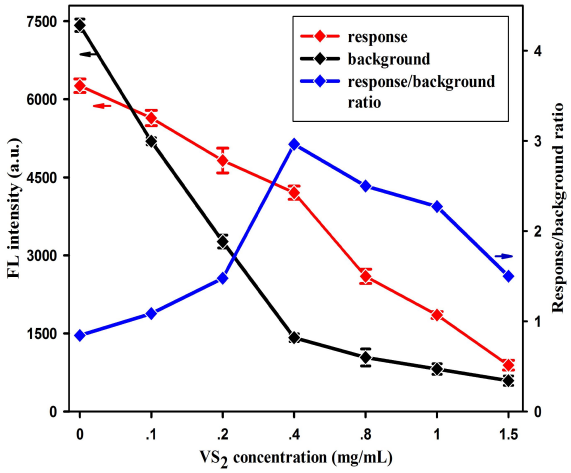

Fig. 4 Fluorescence intensity of P1 (background) and P1- cyt c complex (response) in the presence of VS_2 (0, 0.1, 0.2, 0.4, 0.8, 1.0 and 1.5 mg/mL, 40 μL), P1: 30 μL, 1.5 μM; cyt c: 60 μL, 5×10^{-5} M. Error bars are the standard deviation of three repetitive experiments.

The quantification of cyt c is based on the fluorescence recovery resulted from the formation of P1-cyt c complex (Fig. 1). Both the incubation time of P1 with cyt c and the reaction time of P1 with VS_2 nanosheets would affect the response and were also optimized. Fig. 5A displays the changes in fluorescence intensity of a solution containing 30 μL P1 (1.5 μM) and 60 μL cyt c (5×10^{-5} M) at 518 nm over different incubation time at room temperature. The fluorescence response profiles are shown in the inset of Fig. 5A. One can see that the fluorescence signal decreases to the minimum-value after 10 min incubation, indicating that the reaction between P1 and cyt c is quick and reaches stabilization within only 10 min. Therefore, 10 min was selected as the optimum reaction time of aptamer with cyt c in subsequent experiments.

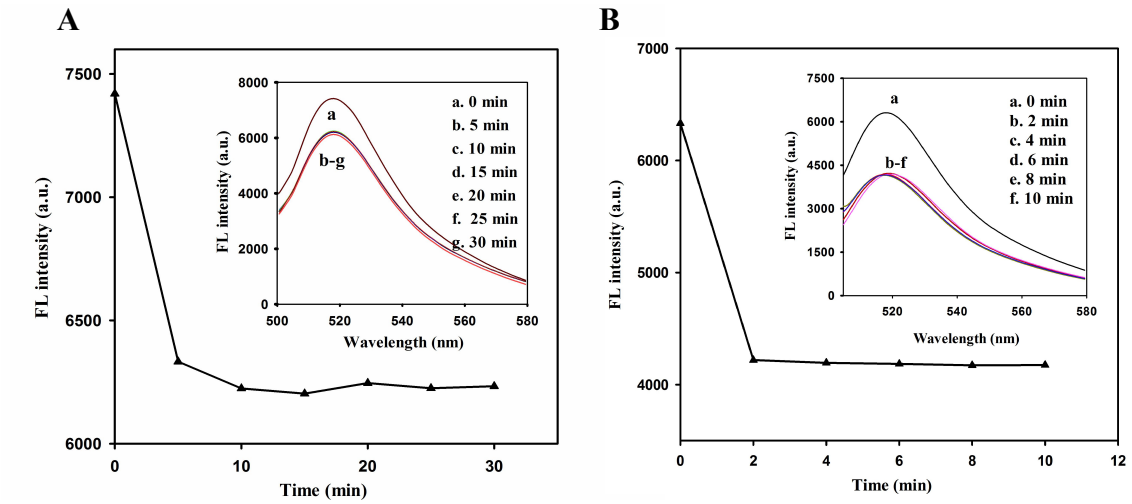

Fig. 5 (A) The dependence of the fluorescence intensity on the incubation time of P1 with cyt c. (B) The dependence of the fluorescence intensity on the incubation time of P1-cyt c complex with VS_2 nanosheet. Inset: the corresponding fluorescence spectra. Excitation and emission wavelengths are at 490 nm and 518 nm, respectively.

Once the P1-cyt c complex was formed (10 min), VS_2 nanosheets were introduced. In this case, the fluorescence intensity depends on the interaction between P1 and cyt c, P1 and VS_2 nanosheet, as well as the P1-cyt c complex and VS_2 nanosheet. Fig. 5B shows the incubation time-dependent change in fluorescence intensity at 518 nm after addition of VS_2 nanosheets into a solution containing aptamer (30 μL, 1.5 μM) and

cyt c (60 μL, 5×10^{-5} M). The response profiles are shown in the inset. One can see that the fluorescence intensity decreases to the minimum within 4 min. Further increasing the incubation time results in no more change in fluorescence, indicating that the interaction of the aptamer-cyt c complex with VS_2 nanosheet is fast and VS_2 nanosheet indeed exhibits good fluorescence quenching stability. Considering a variety of external factors, 5 min was chosen as the optimum incubation time of P1-cyt c complex with VS_2 nanosheet.

Sensitivity of VS_2 nanosheets-based biosensor towards cyt c

Fig. 6 A shows the cyt c concentration-dependent fluorescence responses. In this system, 30 μL P1 (1.5 μM) was incubated with 60 μL cyt c at different concentrations for 10 min, then, 40 μL VS_2 nanosheets solution (0.4 mg/mL) was added. After incubating the solution for another 5 min, the fluorescence responses were detected. The fluorescence was recovered with the addition of cyt c, and the recovery value increases with increasing the cyt c concentrations reaching a plateau after 5×10^{-5} M cyt c. Further increasing the cyt c concentration results in a little increase in the recovery of the fluorescence due to the saturation. Fig. 6 B shows the relationship between the recovery of fluorescence ($F-F_0$, where F_0 and F represent the fluorescence intensity at 518 nm in the absence and presence of cyt c, respectively) and the logarithm of cyt c concentration. A linear response is observed in the range of 0.75 nM to 50 μM, with a correlation coefficient of 0.998, and a regression equation of:

$$F - F_0 = 4724.1 + 452.4\ LogC$$

where C is the concentration of cyt c. In the low or high concentration region, the responses deviate from the linear relationship. The limit of detection (LOD) was defined as 0.5 nM as it can be completely distinguished from the control (Fig. 6A).

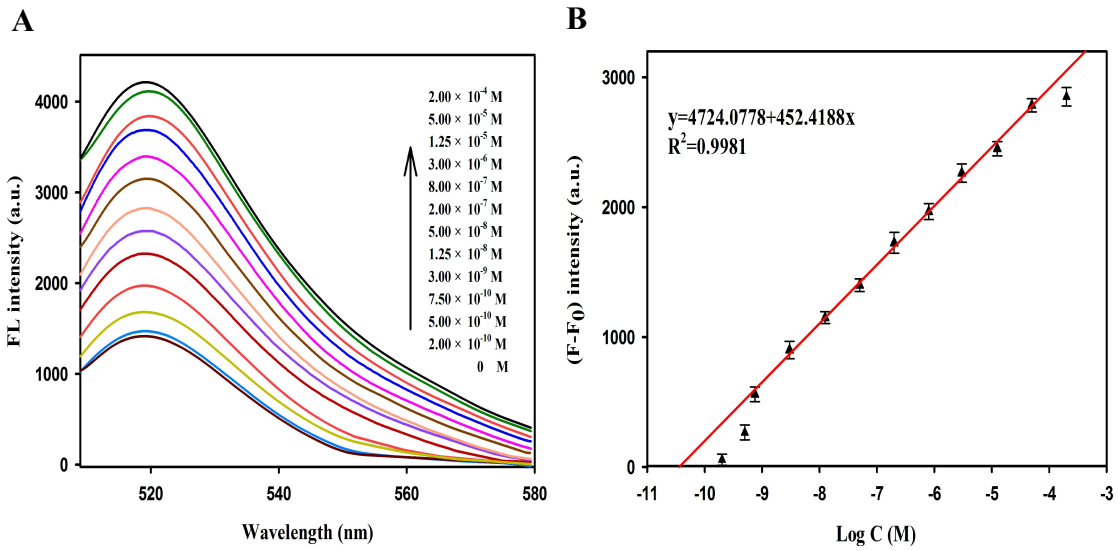

Fig. 6 (A) Responses profiles. (B) The calibration curve. Error bars are the standard deviation of three repetitive experiments. Excitation and emission wavelengths are at 490 nm and 518 nm, respectively.

Selectivity of VS_2 nanosheets-based sensor towards cyt c

It is universally acknowledged that the composition in organisms is rather complicated, so the resistance to interference from irrelevant contaminants is of great importance for a biosensor. To study the specificity of the biosensor, the sensor responses to some related biological species which are widespread in organisms including L-cysteine, L-tyrosine, L-arginine, L-tryptophan, L-valine, Glu, IgG, GSH, BSA, OVA, ascorbic acid and avidin were measured using the same experimental procedures as for cyt c. As shown in Fig. 7, the sensor shows little responses towards all of the tested compounds except cyt c, indicating a high selectivity of the developed method towards cyt c.

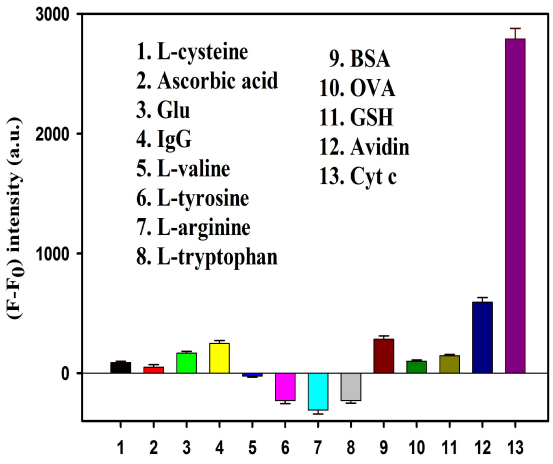

Fig. 7 Fluorescence responses of the sensor towards: (1) L-cysteine, (2) ascorbic acid, (3) Glu, (4) IgG, (5) L-valine, (6) L-tyrosine, (7) L-arginine, (8) L-tryptophan, (9) BSA, (10) OVA, (11) GSH, (12) avidin, and (13) cyt c at concentrations of 5×10^{-5} M. F_0 and F represent the fluorescence intensity at 518 nm in the absence and presence of cyt c, respectively. Error bars are the standard deviation of three repetitive experiments.

Conclusion

For the first time, VS_2 nanosheet was prepared and applied as a sensor platform for the detection of cyt c based on its adsorption and fluorescence quenching ability towards dye-labeled aptamer. The proposed method is relatively simple and fast, the detection can be finished within a few minutes, greatly shorter than the reported aptamer-based methods.[58, 59] Due to the high specificity of the used aptamer, the sensor showed a high selectivity towards cyt c with a LOD of 0.50 nM. As the prepared VS_2 is high-quality and well-dispersed nanosheets, all the assays occur in liquid phase, making it easy to automate and suitable for in situ detection.

Experimental section

Materials and chemicals

Sodium orthovanadate ($Na_3VO_4\cdot12H_2O$) (99.9%), thioacetamide (TAA) (99.0%),

were commercially available from Aladdin (Shanghai, China). Cyt c and the FAM-labeled aptamer: (FAM-5'-CCGTGTCTGGGGCCGACCGGCGC ATTGGGTACGTTGTTGC-3') were purchased from Amresco (U.S.). L-cysteine, L-valine, L-tyrosine, L-arginine, L-tryptophan, glucose (Glu), immunoglobulin (IgG), glutathione (GSH), bull serum albumin (BSA), ovalbumin (OVA), ascorbic acid and avidin were purchased from Sigma-Aldrich Chemical Co. (St. Louis, MO, USA). All other reagents of analytical reagent (AR) grade were obtained from commercial sources and used as received without any further purification.

Aptamer was dissolved in 50 mM Tris-HCl (pH 7.4) containing 20 mM KCl and 600 mM NaCl. Cyt c was dissolved in 50 mM Tris-HCl (pH 7.4) containing 20 mM KCl and 120 mM NaCl.

All experiments, excluding those with special annotation, were conducted at room temperature. All ultrapure water was prepared with Mill-Q water (Millipore, 18.2 MΩ resistivity) and used throughout the experiment.

Apparatus

The morphologies of the prepared materials (precursor $VS_2 \cdot NH_3$ and VS_2 adsorbed on titanium substrate) were analyzed using field-emission scanning electron microscope (FE-SEM, Hitachi S-4800), high-resolution transmission electron microscopy (HRTEM) and transmission electron microscopy (TEM) on a JEM 3010 (JEOL, Japan) electron microscope operating at 200 kV. Energy dispersive X-ray spectrometer (EDS) fitted to the field-emission scanning electron microscope was used to identify elemental composition of the product. Fluorescence spectra were recorded with a Hitachi F-4600 fluorescence spectrophotometer (Tokyo, Japan).

Fabrication of VS_2 nanosheets

The VS_2 nanosheests were synthesized according to the previously reported method with minor modifications.[43]

First, the intermediate intercalated $VS_2 \cdot NH_3$ precursor was prepared by hydrothermal method. Briefly, 3 mmol $Na_3VO_4 \cdot 12H_2O$ and 15 mmol TAA were dissolved in 40 mL ultrapure water in a glass jar to form a homogeneous solution

under stirring. The solution was transferred to a 50 mL Teflon-lined autoclave which was then sealed and heated up to 160 ℃ for 24 h. Afterwards, the system was allowed to cool down to room temperature. Black precipitate ($VS_2 \cdot NH_3$) was finally collected by centrifugation and washed several times with ultrapure water. Of note, the obtained precursor should be instantly used in the following exfoliation procedures without being dried, otherwise the $VS_2 \cdot NH_3$ would decompose into VS_2 flakes and result in lower exfoliation efficiency.

Then, a liquid exfoliating process was conducted. In a typical reaction, 20 mg the as-obtained $VS_2 \cdot NH_3$ was dispersed in 30 mL water in a conical flask, and bubbled with nitrogen to expel the dissolved oxygen away from the solution, avoiding the possible oxidation of V(IV) to V(V). After ultrasonicating the above dispersion in iced water for 3 h, the resultant black suspension was filtered by a medium-speed qualitative paper filter to remove the unexfoliated flakes from the solution, yielding a translucent solution of VS_2 nanosheets.

Pretreatment of aptamer

Prior to the detection of the target, the aptamer solution was heated at 95 ℃ for 5 min and then placed in ice bath immediately for 5 min, followed by cooling at room temperature. The heat treatment was a common practice applied to allow the aptamers to form the desired conformation through renaturation.

Fluorescence detection of cyt c

Then, 30 μL of the as-treated aptamer (P1) (1.5 μM) was incubated with 60 μL of cyt c at different concentrations (ranging from 0 to 2.0×10^{-4} M) at room temperature for 30 min. Then, 40 μL as prepared VS_2 nanosheets solution (0.4 mg/mL) was added and the mixture was incubated at room temperature for 15 min. Afterwards, the fluorescence emission intensity at 518 nm of the mixture was performed with excitation at 490 nm. The kinetic behaviors were studied by monitoring the cyt c-resulted fluorescence recovery.

Acknowledgment

The authors are thankful to the National Science Foundation of China under the grant (21175038, 21235002) for providing financial support.

References

1. Y. L. P. Ow, D. R. Green, Z. Hao and T. W. Mak, *Nat. Rev. Mol. Cell. Bio*., 2008, **9**, 532.
2. M. Hüttemann, P. Pecina, M. Rainbolt, T. H. Sanderson, V. E. Kagan, L. Samavati, J. W. Doan and I. Lee, *Mitochondrion*, 2011, **11**, 369.
3. J. Radhakrishnan, S. Wang, I. M. Ayoub, J. D. Kolarova, R. F. Levine and R. J. Gazmuri, *Am. J. Physiol-heart. C*, 2007, **292**, H767.
4. E. Bossy-Wetzel, D. D. Newmeyer and D. R. Green, *Embo J*., 1998, **17**, 37.
5. M. O. Hengartner, *Nature*, 2000, **407**, 770.
6. M. Christophe and S. Nicolas, *Curr. Pharm. Design*, 2006, **12**, 739.
7. J. C. Martinou, 1999, *Nature*, **399**, 411.
8. D. R. Green and J. C. Reed, *Science-AAAS-Weekly Paper Edition*, 1998, **281**, 1309.
9. S. Morais Cardoso, R. H. Swerdlow and C. R. Oliveira, *Brain Res.*, 2002, **931**, 117.
10. L. L. Gao, F. R. Li, P. Jiao, M. F. Yang, X. J. Zhou, Y. H. Si, W. J. Jiang and T. T. Zheng, *World J. Gastroentero.*, 2011, **17**, 4389.
11. N. J. Waterhouse and J. A. Trapani, *Cell Death Differ.*, 2003, **10**, 853.
12. J. M. Song, P. M. Kasili, G. D. Griffin and T. Vo-Dinh, *Anal. Chem.*, 2004, **76**, 2591.
13. C. B. Campos, B. A. Paim, R. G. Cosso, R. F. Castilho, H. Rottenberg and A. E. Vercesi, *Cytometry Part A*, 2006, **69**, 515.
14. S. N. Tan and L. Hua, *Anal. Chim. Acta*, 2001, **450**, 263.
15. E. D. Crouser, M. E. Gadd, M. W. Julian, J. E. Huff, K. M. Broekemeier, K. A. Robbins and D. R. Pfeiffer, *Analy. Biochem*., 2003, **317**, 67.
16. T. Nakashima and M. Sano, *J. Phys. Chem. C*, 2011, **115**, 20931.
17. C. Vargas, A. G. McEwan and J. A. Downie, *Analy. Biochem.*, 1993, **209**, 323.
18. T. Wang, S. Zhang, C. Mao, J. Song, H. Niu, B. Jin and Y. Tian, *Biosens. Bioelectron.*, 2012, **31**, 369.

19. X. W. Hu, C. J. Mao, J. M. Song, H. L. Niu, S. Y. Zhang, and H. P. Huang, *Biosens. Bioelectron.*, 2013,**41**, 372.
20. G. X. Wang, Y. Qian, X. X. Cao and X. H. Xia, *Electrochem. Commun.*, 2012, **20**, 1.
21. X. W. Hu, C. J. Mao, J. M. Song, H. L. Niu, S. Y. Zhang and H. P. Huang, *Biosens. Bioelectron.*, 2013, **41**, 372.
22. Y. Liu and W. Wei, *Anal. Sci.*, 2008, **24**, 1431.
23. C. H. Lu, H. H. Yang, C. L. Zhu, X. Chen and G. N. Chen, *Angew. Chem.*, 2009, **121**, 4879.
24. H. Chang, L. Tang, Y. Wang, J. Jiang and J. Li, *Anal. Chem.*, 2010, **82,** 2341–2346.
25. P. J. J. Huang and J. Liu, *Anal. Chem.*, 2012, **84**, 4192.
26. H. Dong, J. Zhang, H. Ju, H. Lu, S. Wang, S. Jin, K. H. Hao, H. W. Du and X. Zhang, *Anal. Chem.*, 2012, **84**, 4587.
27. A. D. Yoffe, *Solid State Ionics*, **39**, 1990, 1.
28. A. D. Yoffe, *Springer Berlin Heidelberg, in Festkörperprobleme*, 1973, **13**, 1.
29. N. J. Doran, *Physica B+C*, 1980, **99,** 227.
30. Q. H. Wang, K. Kalantar-Zadeh, A. Kis, J. N. Coleman and M. S. Strano, *Nature Nanotech.*, 2012, **7**, 699.
31. M. Xu, T. Liang, M. Shi and H. Chen, *Chem. Rev.*, 2013, **113**, 3766.
32. X. Huang, Z. Zeng and H. Zhang, *Chem. Soc. Rev.*, 2013, **42**, 1934.
33. S. Z. Butler, S. M. Hollen, L. Cao, Y. Cui, J. A. Gupta, H. R. Gutiérrez, T. F. Heinz, S. S. Hong, J. X. Huang, A. F. Ismach, E. Johnston-Halperin, M. Kuno, V. V. Plashnitsa, R. D. Robinson, R. S. Ruoff, S. Salahuddin, J. Shan, L. Shi, M. G. Spencer, M. Terrones, W. Windl and J. E. Goldberger, *ACS Nano*, 2013, **7**, 2898.
34. M. Chhowalla, H. S. Shin, G. Eda, L. J. Li, K. P. Loh and H. Zhang, *Nature Chem.*, 2013, 5, 263.
35. H. Li, J. Wu, Z. Yin and H. Zhang, *Accounts Chem. Res.*, 2014, **47**,1067.
36. C. Zhu, Z. Zeng, H. Li, F. Li, C. Fan and H. Zhang, *J. Am. Chem. Soc.*, 2013, **135,** 5998.

37. Y. Yuan, R. Li and Z. Liu, *Anal. Chem.*, 2014, **86**, 3610.
38. Q. Xi, D. M. Zhou, Y. Y. Kan, J. Ge, Z. K. Wu, R. Q. Yu and J. H. Jiang, *Anal. Chem.*, 2014, **86**, 1361.
39. D. Li, S. Song and C. Fan, *Accounts Chem. Res.*, 2010, **43**, 631.
40. A. Vallée-Bélisle and K. W. Plaxco, *Curr. Opin. Struc. Biol.*, 2010, **20**, 518.
41. M. Mulazzi, A. Chainani, N. Katayama, R. Eguchi, M. Matsunami, H. Ohashi, Y. Senba, M. Nohara, M. Uchida, H. Takagi and S. Shin, *Phys. Rev. B*, 2010, **82**, 075130.
42. J. Feng, L. Peng, C. Wu, X. Sun, S. Hu, C. Lin, J. Dai, J. Yang and Y. Xie, *Adv. Mater.*, 2012, **24**, 1969.
43. J. Feng, X. Sun, C. Wu, L. Peng, C. Lin, S. Hu, J. Yang and Y. Xie, *J. Am. Chem. Soc.,* 2011,**133**, 17832.
44. H. A. Therese, F. Rocker, A. Reiber, J. Li, M. Stepputat, G. Glasser, U. Kolb and W. Tremel, *Angew. Chem. Int. Edit.*, 2005, **44**, 262.
45. A. V. Murugan, M. Quintin, M. H. Delville, G. Campet and K. Vijayamohanan, *J. Mater. Chem.*, 2005, **15**, 902.
46. Y. Ma, Y. Dai, M. Guo, C. Niu, Y. Zhu and B. Huang, *ACS Nano*, 2012, **6**, 1695.
47. M. Zhong, Y. Li, Q. Xia, X. Meng, F. Wu and J. Li, *Mater. Lett.*, 2014, **124**, 282.
48. D. Q. Gao, Q. X. Xue, X. Z. Mao, W. X. Wang, Q. Xu and D. S. Xue, *J. Mater. Chem. C*, 2013, **1**, 5909.
49. A. P. De Silva, H. N. Gunaratne, T. Gunnlaugsson, A. J. Huxley, C. P. McCoy, J. T. Rademacher and T. E. Rice, *Chem. Rev.*, 1997, **97**, 1515.
50. K. Rurack, *Spectrochim. Acta A*, 2001, **57**, 2161.
51. J. Liu and Y. Lu, *J. Am. Chem. Soc.*, 2007,**129**, 9838.
52. C. Tuerk and L. Gold, *Science*, 1990, **249**, 505.
53. A. D. Ellington and J. W. Szostak, *Nature*, 1990, **346**, 818.
54. A. B. Iliuk, L. Hu and W. A. Tao, *Anal. Chem.*, 2011, **83**, 4440.
55. M. Mascini, I. Palchetti and S. Tombelli, *Angew. Chem. Int. Edit.*, 2012, **51**, 1316.
56. G. Q. Wang, Y. Q. Wang, L. X. Chen and J. Choo, *Biosens. Bioelectron.*, 2010, **25**, 1859.

57. A. J. Groszek, *Nature*, 1964, **204**, 680.

58. J. F. C. Loo, P. M. Lau, H. P. Ho and S. K. Kong, *Talanta*, 2013, **115**, 159.

59. I. P. M. Lau, E. K. S. Ngan, J. F. C. Loo, Y. K. Suen, H. P. Ho and S. K. Kong, *Biochem. Bioph. Res. Co.*, 2010, **395**, 560.